Nucl Med Mol Imaging (2011) 45:203–211
DOI 10.1007/s13139-011-0099-3

ORIGINAL ARTICLE

Evaluation of Bone Metastasis from Hepatocellular Carcinoma Using ^{18}F-FDG PET/CT and ^{99m}Tc-HDP Bone Scintigraphy: Characteristics of Soft Tissue Formation

Hyo Jung Seo · Yun Jung Choi · Hyun Jeong Kim · Yong Hyu Jeong · Arthur Cho · Jae Hoon Lee · Mijin Yun · Hye Jin Choi · Jong Doo Lee · Won Jun Kang

Received: 24 April 2011 / Revised: 19 June 2011 / Accepted: 13 July 2011 / Published online: 5 August 2011

Abstract
Purpose Bone metastasis from hepatocellular carcinoma (HCC) can present with soft tissue formation, resulting in oncologic emergency. Contrast-enhanced FDG PET/CT and bone scintigraphy were compared to evaluate characteristics of bone metastases with or without soft tissue formation from HCC.
Methods Of 4,151 patients with HCC, 263 patients had bone metastases. Eighty-five patients with bone metastasis from HCC underwent contrast-enhanced FDG PET/CT. Fifty-four of the enrolled subjects had recent ^{99m}Tc-HDP bone scintigraphy available for comparison. Metastatic bone lesions were identified with visual inspection on FDG PET/CT, and maximum standardized uptake value (SUV_{max}) was used for the quantitative analysis. Confirmation of bone metastasis was based on histopathology, combined imaging modalities, or serial follow-up studies.
Results Forty-seven patients (55%) presented with soft tissue formation, while the remaining 38 patients presented without soft tissue formation. Frequent sites of bone metastases from HCC were the spine (39%), pelvis (19%), and rib cage (14%). The soft-tissue-formation group had more frequent bone pain (77 vs. 37%, $p<0.0001$), higher SUV_{max} (6.02 vs. 3.52, $p<0.007$), and higher incidence of photon defect in bone scintigraphy (75 vs. 0%) compared to the non-soft-tissue-formation group. FDG PET/CT had higher detection rate for bone metastasis than bone scintigraphy both in lesion-based analysis (98 vs. 53%, $p=0.0015$) and in patient-based analysis (100 vs. 80%, $p<0.001$).
Conclusions Bone metastasis from HCC showed a high incidence of soft tissue formation requiring emergency treatment. Although the characteristic findings for soft tissue formation such as photon defect in bone scintigraphy are helpful in detection, overall detectability of bone metastasis is higher in FDG PET/CT. Contrast-enhanced PET/CT will be useful in finding and delineating soft-tissue-forming bone metastasis from HCC.

Keywords Hepatocellular carcinoma · Fluorodeoxyglucose · Positron emission tomography · Soft tissue formation · Bone metastasis

H. J. Seo · Y. J. Choi · H. J. Kim · Y. H. Jeong · A. Cho · J. H. Lee · M. Yun · J. D. Lee · W. J. Kang (✉)
Division of Nuclear Medicine, Department of Radiology, Yonsei University College of Medicine, Seongsanno250, Seodaemun-gu, Seoul 120-752, Korea
e-mail: mdkwj@yuhs.ac

H. J. Choi
Division of Oncology, Department of Internal Medicine, Yonsei University College of Medicine, Seoul, Korea

Introduction

Hepatocellular carcinoma (HCC) is one of the most common solid malignancies in the world, and its prevalence is higher in Asian countries [1]. HCC accounts for over 80% of all primary liver cancers, which rank fourth among cancer-related deaths worldwide [2]. The incidence of extrahepatic metastases from HCC was reported to be 37% with the following order of frequency: the lung, lymph nodes, and bone [3]. The extrahepatic metastases occur in advanced stages, and an accurate diagnosis of extraheptic metastases is of great value for determining the therapeutic modality at an early stage [4].

Bone metastasis from HCC is not uncommon, and the incidence has been increasing [5, 6]. A recent study reported that patients with isolated bone metastasis showed longer survival than those with metastases in bone and other sites [7]. Meanwhile, bone metastases-associated expansile soft tissue mass and bony destruction can cause clinical emergencies such as severe pain, spinal cord compression, and paralysis. Therefore, immediate operation or radiation therapy should be considered in bone metastasis with soft tissue formation [8–10]. However, the clinical importance of bone metastasis from HCC-originated soft tissue components has been underestimated due to the low incidence in Western countries.

^{99m}Tc-MDP or HDP bone scintigraphy (BS) has been widely used to detect bone metastasis in most malignancies. Due to the osteolytic nature of bone metastasis from HCC, the detectability of BS has been reported to be lower compared with cancers with osteoblastic metastasis [11–13]. Bony destruction resulting from osteolytic metastasis can present with photon defects in BS [14–16], but the correlation with ^{18}F-fluoro-2-deoxy-D-glucose (FDG) PET/CT has not been explored.

FDG PET/CT has been known to be less suitable for primary HCC due to limited detectability [17]. However, several studies reported that PET or PET/CT is useful for detection of extrahepatic metastases from HCC [18–21]. Moreover, PET/CT showed higher sensitivity for the detection of bone metastasis than other extrahepatic metastases from HCC [22]. The aim of the present study is to evaluate the feasibility of FDG PET/CT for assessing bone metastasis from HCC and to describe imaging characteristics of bone metastases from HCC according to the presence of soft tissue formation.

Materials and Methods

Patients

We reviewed 4,151 patients diagnosed with HCC between January 2005 and December 2010. Of the 263 patients confirmed to have bone metastasis, 103 patients underwent contrast-enhanced PET/CT for the evaluation of suspicious bone metastasis and/or other extrahepatic metastasis. In our institute, contrast-enhanced PET/CT is routinely performed in most patients with HCC when extrahepatic metastases are suspected based on laboratory examinations, clinical symptoms, CT, and other imaging modalities. Eighteen patients were excluded from the study for the following reasons: 13 patients had diffuse bone metastases; 2 patients had double primary; and 3 patients were not confirmed as having bone metastasis. Ultimately, a total of 85 patients were included in this study.

Contrast-Enhanced FDG PET/CT

All patients were instructed to fast for 8 h except for glucose-free oral hydration before the PET examination, and the blood glucose concentration was measured and confirmed to be less than 140 mg/dL. Intravenous injections of 5.5 MBq of ^{18}F-FDG per kilogram of body weight were administered. All patients were kept lying comfortably during the 60 min uptake period and voided before being supinely positioned on the scanner table. Integrated FDG PET/CT scanning was performed using a combined PET/CT scanner (Discovery STE; GE Healthcare, Milwaukee, WI). Sixty minutes after the ^{18}F-FDG injection, the first unenhanced CT scan with eight-slice scanner was performed from the vertex of the skull through the mid-thigh using the following parameters: 120 kVp; 30 mA; 0.8 s rotation time; 3.75 mm helical thickness; 27 mm per rotation (speed); 2.5 mm scan reconstruction, with a reconstruction index of 1.25 mm; 15.7 cm field of view; and a 512×512 matrix. A PET scan was then acquired from the level of the ear through the mid-thigh in three-dimensional mode at 2.5 min per bed position. The PET unit had an axial field of view of 50 cm and a spatial resolution of 4.29 mm in full width of half maximum at 1 cm from the center. PET data were reconstructed iteratively using an ordered-subset expectation maximization algorithm. After finishing PET scans, 2 ml/s of contrast medium (Omnipaque 300, GE Healthcare) was injected, and a contrast-enhanced CT scan of the same imaging field was obtained immediately at 120 kVp and 230 mA, with a helical thickness of 3.75 mm, 60 s. The reconstructed CT, PET, and fused PET/CT images were displayed in axial, sagittal, and coronal planes.

Contrast-enhanced PET/CT was interpreted by two experienced nuclear medicine physicians (who had 3–4 years of experience with contrast-enhanced PET/CT) without knowledge of the patient's clinical history. A bone lesion on PET/CT was regarded as bone metastasis if two nuclear medicine physicians agreed that there was abnormally increased FDG uptake compared with background bone marrow and osteolytic/osteoblastic change with/without bony destruction on bone window setting CT.

A region of interest (ROI) was placed over all suspected bone lesions to measure maximum intensity in each lesion for semi-quantitative analysis. The standardized uptake value (SUV) was calculated by using the following formula: radioactivity concentration in the region of interest (Bq/ml)/(injected dose of FDG/body weight in grams). The value of SUV_{max} of metastatic bone lesion was not used for the visual interpretation.

On contrast-enhanced CT as part of PET/CT, the presence of the soft-tissue component was evaluated using CT attenuation values (Hounsfield units). Soft tissue

formation was determined by reviewing nonenhanced and contrast-enhanced CT. Bone destructive lesion with soft tissue density that was well-enhanced by contrast dye was considered soft tissue formation (Fig. 1).

Tc-99m HDP Bone Scintigraphy

Bone scintigraphy was performed using a dual-head gamma camera (ADAC Dual genesys, ADAC Laboratories, Milpitas, CA) equipped with general-purpose collimators. Anterior and posterior whole-body images were acquired approximately 3 h after intravenous administration of 925 MBq ^{99m}Tc-hydroxymethane diphosphonate (HDP). Additional static planar images were acquired at the discretion of the attending nuclear physician. Single photon emission computed tomography was not performed routinely.

Bone scintigraphy was interpreted by two experienced nuclear medicine physicians (who had 3–4 years of experience with bone scintigraphy) without knowledge of the patient's clinical history. A bone lesion on bone scintigraphy was considered as significant if it showed abnormal uptake excluding lesions interpreted as arthritis, osteophytes, or benign compression fracture. A lesion with a central cold defect was considered to be a malignant lesion [23, 24].

Determination of Bone Metastasis

Confirmation of bone metastasis by biopsy was available in 18 patients. All other lesions not confirmed by biopsy were considered to be true-positive findings if at least one of the following criteria was satisfied: (1) serial PET/CT scans (obtained at 3–6 month follow-up; 11 patients) showing increasing lesion size and/or FDG accumulation, (2) positive findings of bone metastasis on concomitant or follow-up MR finding (23 patients), (3) serial CT findings of osteolytic and/or destructive changes (15 patients), (4) osteolytic/osteoblastic lesions with abnormally increased FDG uptake and/or expansile or erosive cortical changes present on contrast-enhanced PET/CT (6 patients), (5) concomitant or follow-up bone scintigraphy findings with bone involvement (22 patients) [7]. Ten patients were confirmed based on more than two criteria.

Statistical Analysis

All data were analyzed using statistical software (Medcalc Software, Mariakerke, Belgium). The mean age of men and women was compared using the independent-sample t test. The χ^2 test was used to compare the patients' background characteristics and symptoms. Survival rate was evaluated by the Kaplan-Meier method, and the log-rank test was used to compare survival rates. An alternative-free response receiver operating characteristic (ROC) curve was analyzed to find the cut-off value of bone metastasis with soft-tissue component. $P<0.05$ was considered statistically significant.

Results

Patient Characteristics

A total of 85 patients were enrolled in the present study (70 male and 15 female patients, mean age 58 years). Among the 85 patients, 47 were diagnosed as having soft tissue formation, and 38 were diagnosed as having no soft tissue formation. Demographic characteristics of each group are displayed in Table 1. Presence of viral infection, serum α-fetoprotein (AFP) level, Child-Pugh class, histopathologic

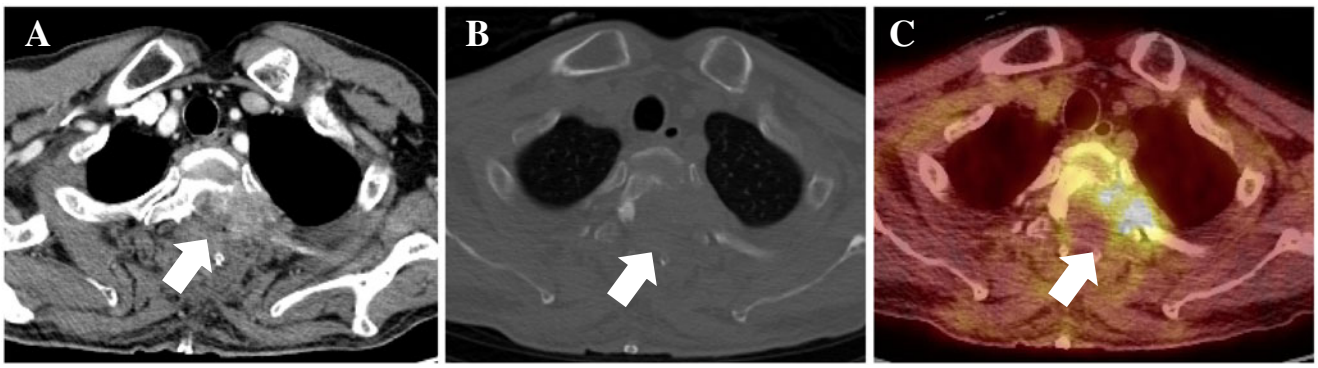

Fig. 1 Determination of soft tissue formation by contrast-enhanced CT, precontrast CT, and FDG PET/CT. A 65-year-old man diagnosed with hepatocellular carcinoma had severe bone pain on T-spine level. **a** Contrast-enhanced CT revealed bone metastasis with soft-tissue component involving T2 and left posterior second rib. This mass compressed the spinal cord and nerve root causing severe pain and paralysis. **b** Precontrast CT of bone window setting showed osteolytic and destructive bony lesion. **c** Hypermetabolism in T2 vertebra and left posterior second rib is well visualized on fused PET/CT. The patient had the T2 vertebra debulked in an emergency operation

Table 1 Characteristics of patients with bone metastasis from hepatocellular carcinoma according to the presence of soft tissue formation

	Soft tissue component		
	Absent	Present	*P* value
Number of patients	38	47	
Gender			
Male	30	40	0.650
Female	8	7	
Age (years)	57 (29–75)	58 (32–82)	0.480
Hepatitis			
B	30	34	0.745
C	3	4	
Non-B and non-C	5	9	
AFP (IU/ml)	11,391 (1–83,000)	15,688 (2–377,768)	0.846
Child-Pugh class			
A	36	43	0.287
B	1	4	
C	1	0	
Bone pain			
Yes	12	36	<0.0001*
No	25	11	
SUV_{max}	3.52±2.74	6.02±3.56	0.007*
Differentiation of primary HCC			
Well differentiated	1	1	0.996
Moderately differentiated	6	7	
Poorly differentiated	7	9	
Not applicable	23	30	
Survival (years)	6.75 (0.4–23)	6.97 (0.4–28)	0.879
Extrahepatic metastasis except bone			
Lung	4	3	0.314
LN	8	5	
Lung and LN	1	2	
Lung and other organ	0	3	
LN and other organ	2	2	
Other organ	3	5	
Total	18	20	
Isolated bone metastasis	20 (53%)	27 (57%)	

Values are number, median (range), or mean ± SD

*Significant difference between two groups ($P<0.05$)

differentiation, combined extrahepatic metastasis, and isolated bone metastasis were compared between the soft-tissue-forming group and non-forming group, but no significant difference was found.

The soft-tissue-forming group showed higher prevalence of bone pain than the non-forming group (37 vs. 77%, $P<0.0001$).

Bone Metastasis Site Distribution

A total of 211 bone metastatic sites were detected. Of 211 sites, 81 lesions (38%) were classified as soft-tissue-forming metastasis. The regional distribution of bone metastatic sites is listed in Table 2. The frequent sites of bone metastasis from HCC were the spine ($n=100$, 48%) , followed by pelvis ($n=40$, 19%) and rib cage ($n=30$, 14%). There was no significant difference in the affected sites between the soft-tissue-forming group and the non-forming group, except for the high frequency of soft-tissue-forming metastasis in the rib cage (Fig. 2).

Detection Rate by FDG PET/CT and ^{99m}Tc-HDP Bone Scintigraphy

Comparison of detection rate between FDG PET/CT and bone scintigraphy was performed in 54 patients who underwent both procedures (Table 3). On a lesion-based analysis, the detection rate of FDG PET/CT was 98% (134/

Table 2 Distribution of bone metastasis sites from hepatocellular carcinoma according to the presence of soft tissue formation

Distribution	Soft tissue component		Total
	Absent	Present	
Cervical spine	8	3	11
Thoracic spine	28	12	40
Lumbar spine	20	11	31
Sacrum	10	8	18
Pelvis	27	13	40
Rib cage	10	20	30
Humerus	2	1	3
Femur	11	4	15
Scapula/clavicle	8	6	14
Skull	2	3	5
Sternum	4	0	4
Total	130	81	211

137). FDG PET/CT detected all the lesions in the soft-tissue-forming group (detection rate 100%, 53/53). Three lesions without soft tissue components were missed on FDG PET/CT. On bone scintigraphy, 73 lesions were detected (detection rate 53%, 73/137) regardless of soft-tissue components. Missed lesions on bone scintigraphy were mostly bone marrow lesions (n=37) and small lesions with a soft-tissue component less than 3 cm in diameter (n=12). The detection rate of FDG PET/CT was significantly higher than that of bone scintigraphy (P<0.001). There was no statistically significant difference in detection rate according to the presence of soft tissue formation.

Table 3 Comparison of the detection rate [detected lesions/total lesions (%)] between ^{18}F-FDG PET/CT and ^{99m}Tc-HDP bone scintigraphy to reveal bone metastasis from HCC

	PET/CT	Bone scintigraphy	P
Lesion-based analysis			
Soft tissue absent	81/84 (96%)	45/84 (54%)	<0.001*
Soft tissue present	53/53 (100%)	28/53 (53%)	<0.001*
Total	134/137(98%)	73/137(53%)	<0.001*
Patient-based analysis			
Soft tissue absent	24/24 (100%)	16/24 (67%)	0.007*
Soft tissue present	30/30 (100%)	27/30 (90%)	0.236
Total	54/54 (100%)	43/54 (80%)	0.0015*

*Significant difference between two groups (P<0.05)

On a patient-based analysis, FDG PET/CT had an overall higher detection rate than bone scintigraphy

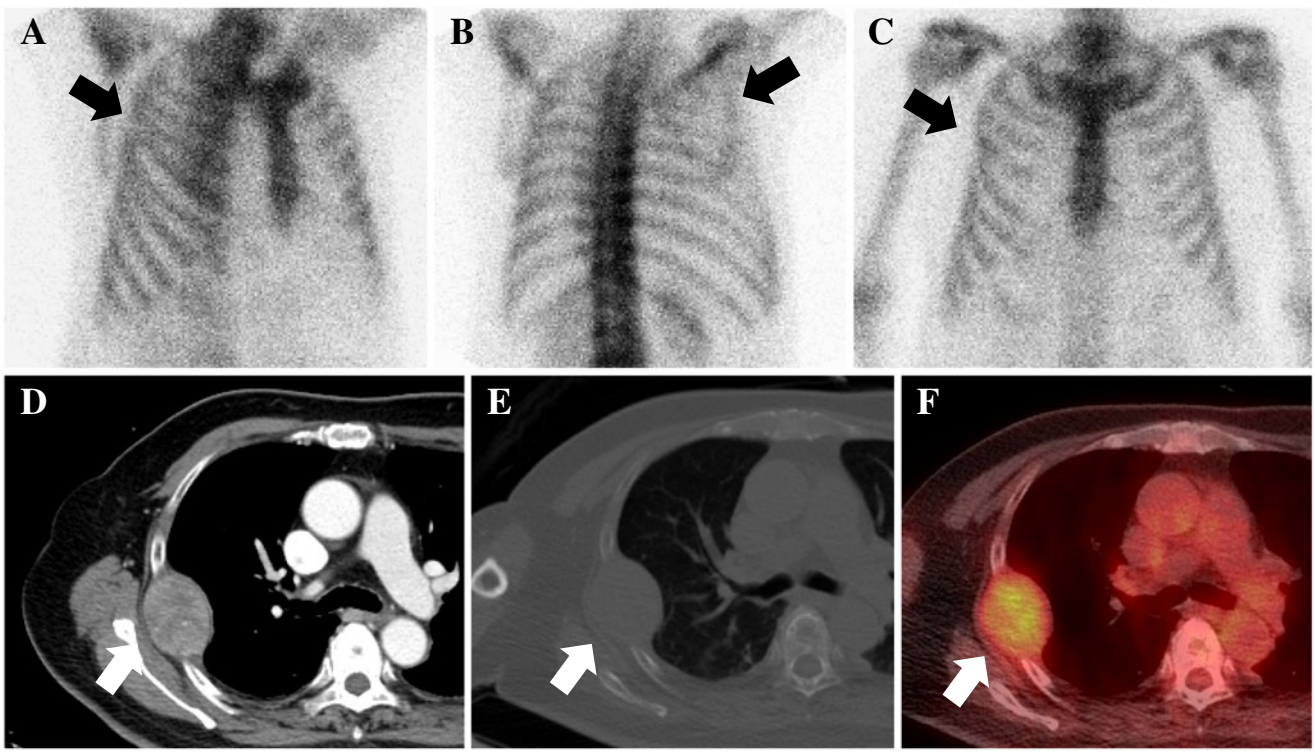

Fig. 2 A 73-year-old man with hepatitis C virus diagnosed with hepatocellular carcinoma with severe bone pain in the right rib cage. **a–c** Bone scintigraphy failed to detect the bone metastasis. **d** Contrast-enhanced CT as part of FDG PET/CT revealed bone metastasis with well-marginated soft-tissue mass involving the axillary portion of the right fourth rib. **e** Precontrast CT of bone window setting showed mass lesion encasing the right fourth rib. **f** Hypermetabolism in the right fourth rib is well visualized on fused PET/CT

(detection rate, 100 vs. 80%), but the difference was significant only in the non-soft-tissue-forming group.

Diagnostic Value of Mean SUV_{max}

SUV_{max} was significantly higher in the soft-tissue-forming group than the non-forming group (Fig. 3, 6.02±3.58 vs. 3.52±2.37). ROC curve revealed the cut-off value of 3.7 SUV_{max} to predict a soft-tissue component but did not reach statistical significance (area under curve 0.723, sensitivity 66.7%, and specificity 68.5%).

Photon Defect on ^{99m}Tc-HDP Bone Scintigraphy

Typical ^{99m}Tc-HDP bone scintigraphic finding suggestive of soft tissue formation was defined as photon defect with marginal increased uptake (Fig. 4). Of the 28 soft tissue lesions, typical findings were detected in 21 lesions on bone scintigraphy (75%), and the most frequent sites were rib cage and spine (Tables 4, 5).

Discussion

The incidence of HCC is increasing in countries where hepatitis B or C virus is endemic [6]. The present study enrolled a relatively large number of patients with bone metastases from HCC and showed better detectability of FDG PET/CT than bone scintigraphy. In addition, we focused on the high prevalence of soft-tissue-forming metastasis in HCC, which is consistent with previous reports [8, 10, 25].

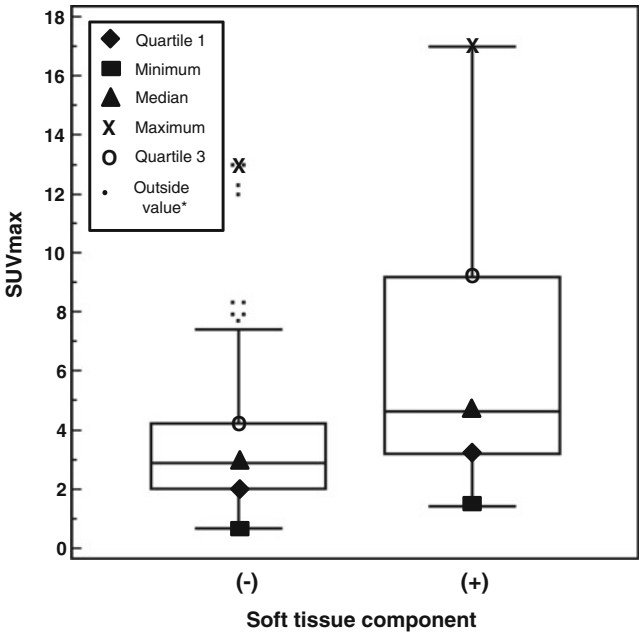

Fig. 3 Box plots show the distribution of SUV_{max} in the bone metastasis groups according to the presence of a soft tissue component. The mean (SD) SUV_{max} was 3.52±2.37 for the bone metastasis group without a soft tissue component and 6.02±3.58 for bone metastasis group with a soft tissue component ($p<0.001$). *Outside value** indicates a value that is larger than the upper quartile plus 1.5 times the interquartile range

The incidence of bone metastasis in HCC has been reported to be 6–10% [7, 26]. The relatively low frequency of bone metastasis from HCC is thought to be related to the fact that most bone metastatic lesions from HCC are osteolytic metastases, which could be missed with conventional bone scintigraphy [27]. However, because FDG PET evaluates the tumor cells in bone metastatic lesions rather than osteoblastic reaction, it is expected to be more sensitive than bone scintigraphy. The incidence of bone metastasis measured by FDG PET in our study was 5.5%, which is consistent with the incidences in the literature. However, one recent study reported that the frequency of bone metastasis from HCC was 19% [7], therefore more studies enrolling larger study groups will be needed to assess the prevalence of bone metastasis from HCC.

Bone metastasis from HCC has the unique characteristic of a high incidence of soft tissue formation. Fukutomi et al. reported that 24 out of 29 lesions (83%) showed osteolysis with expansile soft tissue formation [5]. Kim et al. reported 54% of HCC cases showed soft tissue formation [28], and our study showed 55% of HCC cases showed soft tissue formation on patient-based analysis. Despite the relatively low incidence of bone metastasis, soft tissue formation requiring emergency treatment is frequently observed in HCC, and imaging studies to assess soft tissue formation can be of great clinical importance. Although patients with bone metastasis had markedly elevated AFP, the levels of AFP were not significantly different between the soft-tissue-forming group and the non-forming group in this study. Clinically, the soft-tissue-forming group suffered more bone pain and had higher SUV levels than the non-forming group. According to the results of this study, it is recommended that lesions with symptomatic pain and high SUV level on FDG PET should be carefully examined to determine the presence of soft tissue formation.

^{99m}Tc-MDP or HDP bone scintigraphy has been widely used as a diagnostic modality for screening patients with suspicious metastatic bone disease from various malignancies for decades. However, osteolytic lesions may not be detected on bone scintigraphy, and it has been known to be the pitfall of bone scintigraphy [25, 29]. In this study, all bone metastases from HCC were osteolytic, and the detection rate of bone scintigraphy was low. As is well-known, the detection rate of bone scintigraphy for HCC is much lower than those of breast cancer [11] and lung cancer [30]. However, the characteristic findings of photon defects in soft-tissue-forming lesions can be helpful when

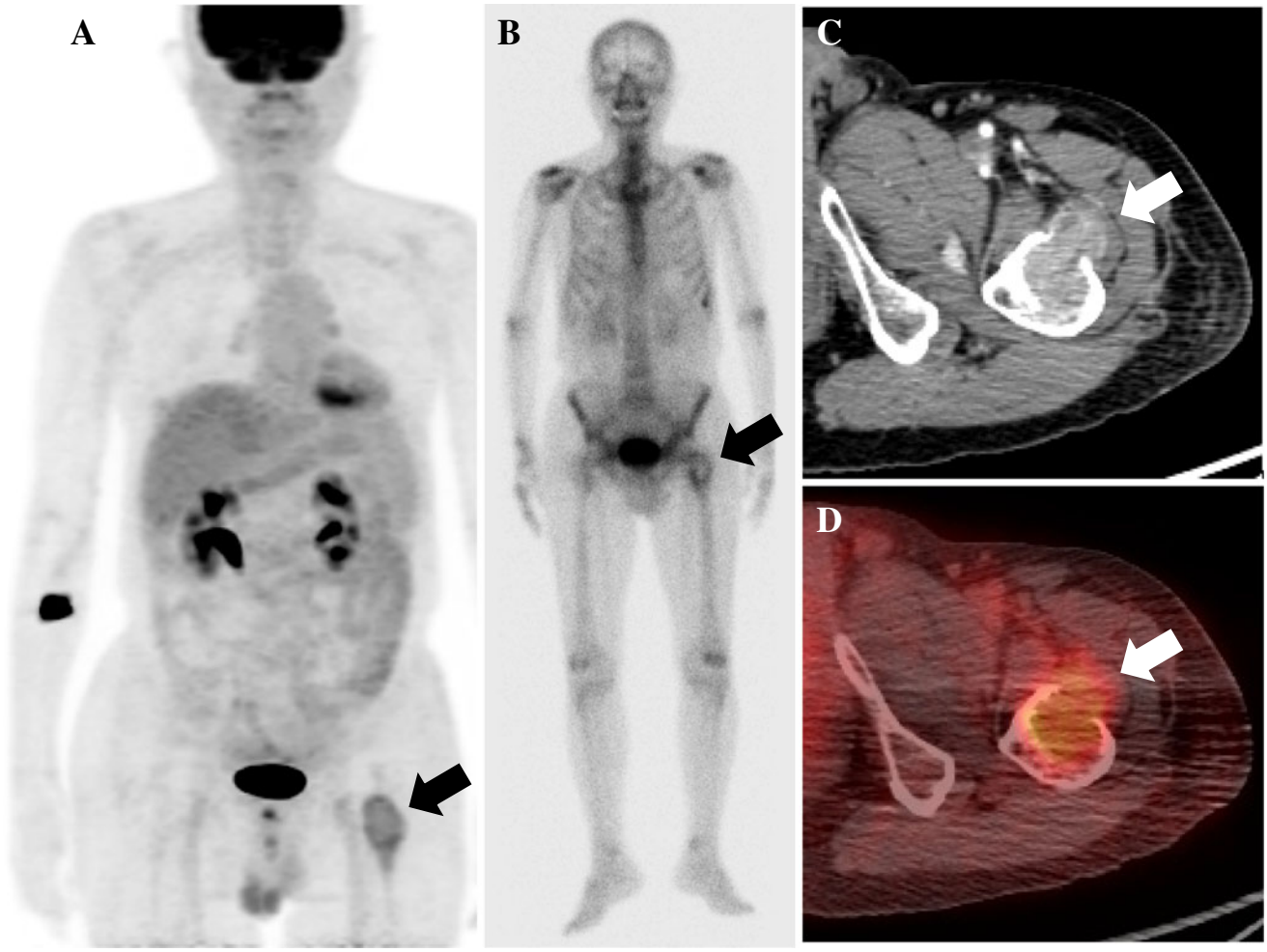

Fig. 4 A 72-year-old man diagnosed with hepatocellular carcinoma with a history of transarterial catheter embolization. During follow-up, the patient complained of bone pain in the left proximal femur with elevated AFP (6,911.73 IU/ml). **a** PET/CT showed increased FDG uptake at the left proximal femur. **b** Whole-body bone scintigraphy shows bone metastasis with photon defect with marginal increased HDP uptake at left proximal femur. Another focal uptake at the costochondral junction of the left eighth rib was a traumatic lesion. **c–d** Axial view of contrast-enhanced CT and PET/CT shows the bone metastasis with soft tissue component at the left proximal femur

Table 4 Distribution of photon defect on ^{99m}Tc-HDP bone scintigraphy

Distribution	Photon defect with marginal increased uptake
Cervical spine	1
Thoracic spine	1
Lumbar spine	1
Sacrum	3
Pelvis	4
Rib cage	5
Scapula	2
Femur	2
Skull	1
Total	21

evaluated for osteolytic metastasis in bone scintigraphy. In this study, photon defect was frequently found on soft-tissue-forming lesions with an incidence of 75%. Photon defect is a well known finding on bone scintigraphy that can be observed in osteolytic metastasis [14–16], and we demonstrated that photon defect on bone scintigraphy in

Table 5 Comparison of bone metastasis with/without soft tissue formation according to findings of ^{99m}Tc-HDP bone scintigraphy

Finding of bone scintigraphy	Soft tissue component	
	Absent	Present
Photon defect with marginal increased uptake	0 (0%)	21 (75%)
Abnormally increased uptake	45 (100%)	7 (25%)
Total	45	28

HCC is directly related to a high prevalence of soft tissue formation.

Overall, the detection rate of FDG PET was superior to bone scintigraphy in the present study. FDG PET has limitations for the diagnosis of primary HCC because of high levels of glucose-6-phosphatase in HCCs, especially in well-differentiated tumors [31–33]. Only a few studies have assessed the diagnostic accuracy of FDG PET in bone metastasis from HCC [34]. Although this study compared detection rates of FDG PET and whole-body bone scintigraphy in selected patients with known bone metastasis, the overall diagnostic accuracy is expected to be higher in FDG PET than bone scintigraphy. Three lesions missed on FDG PET/CT were all pure osteolytic without increased FDG uptake, probably due to recent chemotherapy.

We found in our study that 47 out of 85 (55%) of our patients had isolated bone metastasis, which is consistent with a previous study by Ho et al. They reported that isolated bone metastasis in HCC might not be as uncommon as previously believed, and more common than metastasis to other regions [7]. As is well known, whole body screening with FDG PET or bone scintigraphy is crucial in screening for bone metastasis, and these imaging studies should be considered even in patients without other soft tissue metastasis.

In the present study, six patients with soft tissue formation underwent emergency operation due to impending cord compression and paralysis (data not presented). Non-contrast CT as part of PET/CT can find the destruction of cortex but is limited in delineating the expanding pattern escaping from bone. FDG uptake on soft tissue lesion detected on nonenhanced CT might be the clue to soft-tissue formation. Furthermore, contrast-enhanced CT is routinely performed in most oncologic PET/CT studies in our institute and was performed in all the patients enrolled in this study. Contrast-enhanced CT was especially useful for the evaluation of the extension to the nerve and adjacent tissue, which could be a guideline for further studies including MRI and for the treatment plan.

There were several limitations in this study. Not all of the lesions were confirmed by histopathology. However, this is a well-known limitation of most studies assessing bone metastases, and a clinical decision can be made without pathology confirmation when typical imaging findings are present [3]. Second, the study group comprised a heterogeneous group of patients for staging and follow-up. Forty-four of them had previous treatment history of radiotherapy, chemotherapy, liver resection, transcatheter arterial infusion chemotherapy, and/or radiofrequency ablation therapy. This can be a limitation of evaluation of bone metastasis. Third, only subjects who underwent FDG PET/CT were selected from a total of 263 patients diagnosed with bone metastasis from HCC. Possible selection bias cannot be excluded.

In conclusion, the incidence of bone metastases from HCC is not uncommon, and high incidence of soft tissue formation has unique imaging and clinical characteristics. Although FDG PET was superior to bone scintigraphy in the detection of bone metastasis, bone scintigraphy could be used for screening and for identifying soft-tissue-forming metastasis. Detection of expanding soft tissue lesions on nonenhanced CT, high FDG uptake on areas of soft tissue density, and photon defect on bone scintigraphy were considered as possible indicators of soft-tissue-forming bone metastasis, and enhanced CT for identification of enhancing mass lesions could aid in diagnosis.

Acknowledgments This study was supported by a faculty research grant of Yonsei University for 6-2007-0153.

References

1. Schafer DF, Sorrell MF. Hepatocellular carcinoma. Lancet. 1999;353:1253–7.
2. Park JW. Hepatocellular carcinoma in Korea: introduction and overview. Korean J Gastroenterol. 2005;45:217–26.
3. Katyal S, Oliver 3rd JH, Peterson MS, Ferris JV, Carr BS, Baron RL. Extrahepatic metastases of hepatocellular carcinoma. Radiology. 2000;216:698–703.
4. Vogl TJ, Eichler K, Zangos S, Mack M, Hammerstingl R. Hepatocellular carcinoma: role of imaging diagnostics in detection, intervention and follow-up. Rofo. 2002;174:1358–68.
5. Fukutomi M, Yokota M, Chuman H, Harada H, Zaitsu Y, Funakoshi A, et al. Increased incidence of bone metastases in hepatocellular carcinoma. Eur J Gastroenterol Hepatol. 2001;13:1083–8.
6. Natsuizaka M, Omura T, Akaike T, Kuwata Y, Yamazaki K, Sato T, et al. Clinical features of hepatocellular carcinoma with extrahepatic metastases. J Gastroenterol Hepatol. 2005;20:1781–7.
7. Ho C-L, Chen S, Cheng TKC, Leung YL. PET/CT characteristics of isolated bone metastases in hepatocellular carcinoma. Radiology. 2010;258:515–23.
8. Doval DC, Bhatia K, Vaid AK, Pavithran K, Sharma JB, Hazarika D, et al. Spinal cord compression secondary to bone metastases from hepatocellular carcinoma. World J Gastroenterol. 2006;12:5247–52.
9. Nakamura N, Igaki H, Yamashita H, Shiraishi K, Tago M, Sasano N, et al. A retrospective study of radiotherapy for spinal bone metastases from hepatocellular carcinoma (HCC). Jpn J Clin Oncol. 2007;37:38–43.
10. Lucarini S, Fortier M, Leaker M, Chhem R. Hepatocellular carcinoma bone metastasis in an 11-year-old boy. Pediatr Radiol. 2008;38:111–4.
11. Abe K, Sasaki M, Kuwabara Y, Koga H, Baba S, Hayashi K, et al. Comparison of 18FDG-PET with 99mTc-HMDP scintigraphy for the detection of bone metastases in patients with breast cancer. Ann Nucl Med. 2005;19:573–9.
12. Cook GJ, Houston S, Rubens R, Maisey MN, Fogelman I. Detection of bone metastases in breast cancer by 18FDG pet: differing metabolic activity in osteoblastic and osteolytic lesions. J Clin Oncol. 1998;16:3375–9.
13. Hidaka H, Ishino Y, Nakayama C, Nakata H, Okamura T. Bone scintigraphy in bone metastases due to prostatic cancer. J UOEH. 1987;9:369–77.

14. Momoji J, Shimabukuro H, Higa T, Toda T. A rare case of cranial metastasis from hepatocellular carcinoma. Neurol Surg. 1995;23:997–1002.
15. Leung CMY, Stewart IET, Metreweli C. Simultaneous hot and cold bone scan metastases in hepatocellular carcinoma. Clin Nucl Med. 1995;20:839.
16. Hirano T, Otake H, Kanuma M, Mogi Y, Tatezawa T. Scintigraphic 'doughnut sign' on bone scintigraphy secondary to metastatic hepatocellular carcinoma. Clin Nucl Med. 1995;20:1020–1.
17. Bohm B, Voth M, Geoghegan J, Hellfritzsch H, Petrovich A, Scheele J, et al. Impact of positron emission tomography on strategy in liver resection for primary and secondary liver tumors. J Cancer Res Clin Oncol. 2004;130:266–72.
18. Sugiyama M, Sakahara H, Torizuka T, Kanno T, Nakamura F, Futatsubashi M, et al. 18F-FDG PET in the detection of extrahepatic metastases from hepatocellular carcinoma. J Gastroenterol. 2004;39:961–8.
19. Nagaoka S, Itano S, Ishibashi M, Torimura T, Baba K, Akiyoshi J, et al. Value of fusing PET plus CT images in hepatocellular carcinoma and combined hepatocellular and cholangiocarcinoma patients with extrahepatic metastases: preliminary findings. Liver Int. 2006;26:781–8.
20. Sun L, Guan YS, Pan WM, Luo ZM, Wei JH, Zhao L, et al. Metabolic restaging of hepatocellular carcinoma using whole-body F-FDG PET/CT. World J Hepatol. 2009;1:90–7.
21. Kim YK, Lee KW, Cho SY, Han SS, Kim SH, Kim SK, et al. Usefulness 18F-FDG positron emission tomography/computed tomography for detecting recurrence of hepatocellular carcinoma in posttransplant patients. Liver Transpl. 2010;16:767–72.
22. Kawaoka T, Aikata H, Takaki S, Uka K, Azakami T, Saneto H, et al. FDG positron emission tomography/computed tomography for the detection of extrahepatic metastases from hepatocellular carcinoma. Hepatol Res. 2009;39:134–42.
23. Kruger S, Buck AK, Mottaghy FM, Hasenkamp E, Pauls S, Schumann C, et al. Detection of bone metastases in patients with lung cancer: 99mTc-MDP planar bone scintigraphy, 18F-fluoride PET or 18F-FDG PET/CT. Eur J Nucl Med Mol Imaging. 2009;36:1807–12.
24. Krasnow AZ, Hellman RS, Timins ME, Collier BD, Anderson T, Isitman AT. Diagnostic bone scanning in oncology. Semin Nucl Med. 1997;27:107–41.
25. He J, Zeng ZC, Tang ZY, Fan J, Zhou J, Zeng MS, et al. Clinical features and prognostic factors in patients with bone metastases from hepatocellular carcinoma receiving external beam radiotherapy. Cancer. 2009;115:2710–20.
26. Si MS, Amersi F, Golish SR, Ortiz JA, Zaky J, Finklestein D, et al. Prevalence of metastases in hepatocellular carcinoma: risk factors and impact on survival. Am Surg. 2003;69:879–85.
27. Even-Sapir E. Imaging of malignant bone involvement by morphologic, scintigraphic, and hybrid modalities. J Nucl Med. 2005;46:1356–67.
28. Kim S, Chun M, Wang H, Cho S, Oh YT, Kang SH, et al. Bone metastasis from primary hepatocellular carcinoma: characteristics of soft tissue formation. Cancer Res Treat. 2007;39:104–8.
29. Kuhlman JE, Fishman EK, Leichner PK, Magid D, Order SE, Siegelman SS. Skeletal metastases from hepatoma: frequency, distribution, and radiographic features. Radiology. 1986;160:175–8.
30. Cheran SK, Herndon 2nd JE, Patz Jr EF. Comparison of whole-body FDG-PET to bone scan for detection of bone metastases in patients with a new diagnosis of lung cancer. Lung Cancer. 2004;44:317–25.
31. Okazumi S, Isono K, Enomoto K, Kikuchi T, Ozaki M, Yamamoto H, et al. Evaluation of liver tumors using fluorine-18-fluorodeoxyglucose PET: characterization of tumor and assessment of effect of treatment. J Nucl Med. 1992;33:333–9.
32. Khan MA, Combs CS, Brunt EM, Lowe VJ, Wolverson MK, Solomon H, et al. Positron emission tomography scanning in the evaluation of hepatocellular carcinoma. J Hepatol. 2000;32:792–7.
33. Trojan J, Schroeder O, Raedle J, Baum RP, Herrmann G, Jacobi V, et al. Fluorine-18 FDG positron emission tomography for imaging of hepatocellular carcinoma. Am J Gastroenterol. 1999;94:3314–9.
34. Ho CL, Chen S, Yeung DW, Cheng TK. Dual-tracer PET/CT imaging in evaluation of metastatic hepatocellular carcinoma. J Nucl Med. 2007;48:902–9.